

1 Conservation of *Nematocida* microsporidia gene expression and host response in 2 *Caenorhabditis* nematodes

3
4 Yin Chen Wan¹, Emily R. Troemel², Aaron W. Reinke^{1#}

5
6 ¹ Department of Molecular Genetics, University of Toronto, Toronto, ON, Canada.

7 ² School of Biological Sciences, University of California, San Diego, La Jolla, California, United
8 States of America.

9
10 #Author for Correspondence: Aaron W. Reinke, Department of Molecular Genetics, University
11 of Toronto, Toronto, ON, Canada, 416-946-0889, aaron.reinke@utoronto.ca

12 13 Abstract

14 Microsporidia are obligate intracellular parasites that are known to infect most types of
15 animals. Many species of microsporidia can infect multiple related hosts, but it is not known if
16 microsporidia express different genes depending upon which host species is infected or if the
17 host response to infection is specific to each microsporidia species. To address these
18 questions, we took advantage of two species of *Nematocida* microsporidia, *N. parisii* and *N.*
19 *ausubeli*, that infect two species of *Caenorhabditis* nematodes, *C. elegans* and *C. briggsae*.
20 We performed RNA-seq at several time points for each host infected with either microsporidia
21 species. We observed that *Nematocida* transcription was largely independent of its host. We
22 also observed that the host transcriptional response was similar when infected with either
23 microsporidia species. Finally, we analyzed if the host response to microsporidia infection was
24 conserved across host species. We observed that although many of the genes upregulated in
25 response to infection are not direct orthologs, the same expanded gene families are
26 upregulated in both *Caenorhabditis* hosts. Together our results describe the transcriptional
27 interactions of *Nematocida* infection in *Caenorhabditis* hosts and demonstrate that these
28 responses are evolutionarily conserved.
29

30 **Key words:** *Nematocida* microsporidia, *Caenorhabditis* nematodes, immunity, transcriptional
31 response, host-pathogen interactions

32 Significance statement

33 Microsporidia are a powerful model to study pathogen evolution, but much is still unknown
34 about how these pathogens have evolved to infect multiple host species. We found that
35 microsporidia express most of their genes similarly even when they are infecting different host
36 species and that related host species respond similarly to different microsporidia. Our results
37 suggests that there are conserved transcriptional responses during microsporidia infection.

38 Introduction

39 Microsporidia are obligate eukaryotic intracellular pathogens (Vávra and Lukeš, 2013). This
40 fungal-related phylum contains over 1400 described species that infect a wide range of animal
41 hosts including invertebrates, vertebrates, and protists (Stentiford *et al.*, 2016; Bojko *et al.*,
42 2022). Although as a phylum microsporidia infect a wide range of hosts, most species only
43 infect one or several closely related hosts (Murareanu *et al.*, 2021; Willis and Reinke, 2022).
44 Throughout evolution, microsporidia have lost many metabolic and biosynthesis genes which
45 are present in other eukaryotes (Nakjang *et al.*, 2013). These adaptations to survive within
46 their hosts have resulted in microsporidia having the smallest known eukaryotic genomes
47 (Katinka *et al.*, 2001). These features of microsporidia being able to specifically infect most
48 types of animals with a limited coding capacity have made microsporidia a powerful model for
49 understanding the evolution of intracellular parasites (James *et al.*, 2013; Haag *et al.*, 2014;
50 Quandt *et al.*, 2017; Wadi and Reinke, 2020).

51
52 The model nematode *Caenorhabditis elegans* has become an important system for studying
53 microsporidia infections (Teclé and Troemel, 2022). *Nematocida parisii* and *Nematocida*
54 *ausubeli* (referred to as *Nematocida* sp. 1 in some publications) are the two microsporidia
55 species most commonly observed to infect *Caenorhabditis elegans* (Zhang *et al.*, 2016).
56 These two species of *Nematocida* are also commonly found to infect *Caenorhabditis briggsae*,
57 which has been developed as a comparative species to *C. elegans* (Stein *et al.*, 2003). These
58 two nematode species live in distinct, but overlapping geographical locations (Barrière and
59 Félix, 2005). *N. parisii* was first found infecting *C. elegans* outside of Paris and *N. ausubeli*
60 was originally found infecting *C. briggsae* in India (Troemel *et al.*, 2008). Since then, both
61 microsporidia species have been found infecting both hosts in Europe (Zhang *et al.*, 2016).
62 There are some similarities of infection shared between these two *Nematocida* species; they
63 both exclusively infect the intestine, cause intestinal cells to fuse, and have similar life cycles
64 (Balla *et al.*, 2016). Both species also use similar types of secreted and membrane bound
65 proteins to interface with host proteins (Reinke *et al.*, 2017). There are also differences in their
66 infection characteristics, such as *N. ausubeli* displaying faster growth and increased
67 impairment of host fitness (Balla *et al.*, 2016).

68
69 In response to microsporidia infection, hosts often display large transcriptional changes. The
70 gene expression of *C. elegans* in response to *N. parisii* infection is reported to be distinct from
71 responses to extracellular pathogens, but similar to nodavirus infection (Bakowski *et al.*, 2014).
72 This transcriptional response has been termed the intracellular pathogen response (IPR)
73 (Reddy *et al.*, 2017). Among upregulated IPR genes, many contain F-box, FTH, and MATH
74 domains that are implicated in substrate recognition during ubiquitin-mediated degradation
75 (Thomas, 2006; Bakowski *et al.*, 2014). The IPR also includes upregulation of several
76 *Caenorhabditis* specific families that are still poorly understood, such as the PALS family
77 (Leyva-Díaz *et al.*, 2017). Mutants that cause the IPR to be upregulated are resistant to
78 infection and can clear *N. parisii* infections (Reddy *et al.*, 2019; Teclé *et al.*, 2021; Willis *et al.*,
79 2021).

80
81 Studies looking at infection of nematodes by different bacterial and fungal pathogens showed
82 both significant overlap between pathogen infections, as well as species-specific responses
83 (Wong *et al.*, 2007; Engelmann *et al.*, 2011; Lansdon, Carlson and Ackley, 2022). In addition,
84 recognition of two species of oomycete displayed a shared transcriptional response (Grover
85 *et al.*, 2021). Similarities of responses between different host species have also been observed.
86 For example the response to nodavirus infection is conserved between *C. elegans* and *C.*
87 *briggsae* (Chen *et al.*, 2017). An intergenerational transcriptional response to *Pseudomonas*
88 *vranovensis* was conserved between some, but not all species of *Caenorhabditis* (Burton *et*
89 *al.*, 2021). A study looking at different species of bacterial infection in the nematode
90 *Pristionchus pacificus* also showed both similarities and differences between the
91 transcriptional responses in the two hosts (Sinha *et al.*, 2012). Although conservation of
92 responses between pathogen and hosts in *C. elegans* is observed, different strains of bacteria
93 can elicit different responses, and different strains of *C. elegans* can have distinct responses
94 (Zárate-Potes *et al.*, 2020; Lansdon, Carlson and Ackley, 2022).

95
96 To determine the extent that microsporidia gene expression is influenced by its host and how
97 conserved the host response is to microsporidia infection, we generated and analysed
98 transcriptional data of *N. parisii* and *N. ausubeli* infecting *C. elegans* and *C. briggsae*. We
99 observe similar transcriptional patterns of each *Nematocida* species in the two species of
100 hosts with only a small set of differentially regulated genes. The host response to either of the
101 two microsporidia species was also similar. This transcriptional response is conserved across
102 host species. Altogether, our results suggest that different *Nematocida* species do not have
103 distinct expression programs depending on the host, and transcriptional responses of
104 *Caenorhabditis* hosts to *Nematocida* infection are conserved.

105

106
107
108
109
110
111
112
113
114
115
116
117
118
119
120
121
122
123
124
125
126
127
128
129
130
131
132
133
134
135
136
137
138
139
140
141
142
143
144
145
146
147
148
149
150
151
152
153
154
155
156
157
158
159
160

Results

Gene expression of *N. parisii* and *N. ausubeli* is similar in *C. elegans* and *C. briggsae*

To understand how gene expression of related microsporidia and hosts species is conserved, we infected *Caenorhabditis* nematodes with *Nematocida* microsporidia (fig. 1A). We designed our infection experiment to compare transcriptional differences between related microsporidia and host species (fig. 1B). Unlike previous transcriptional profiling experiments of *Nematocida* infection which were done as continuous infections (Bakowski *et al.*, 2014; Chen *et al.*, 2017), we infected the worms for a short period of time to synchronize the infection. We pulse-infected *C. elegans* and *C. briggsae* with either *N. parisii*, *N. ausubeli*, or a mock treatment for 2.5 hours, washed to remove spores from outside the worms, and then replated the animals for a total of 10, 20, or 28 hours of infection. Each condition was done once, except for the 10-hour time point which was performed in duplicate (fig. 1A). Samples were stained using a probe specific to the *Nematocida* 18S rRNA and we observed that greater than 75% of each population was infected (figs. 2A and B). Compared to *N. parisii*-infected animals, we observed more parasite in *N. ausubeli*-infected hosts at 28 hours, consistent with a previous report that *N. ausubeli* grows faster (Balla *et al.*, 2016). RNA from infected and uninfected animals was extracted and sequenced. To determine the expression of microsporidia genes, we mapped reads of *N. parisii* and *N. ausubeli* to their respective genomes (Supplementary table S1). At 10 hours post infection, the overall percentage of reads from either *N. parisii* or *N. ausubeli* were <1%, which increased to ~3-5% at 28 hours post infection (fig. 2C).

To define the transcriptional patterns of *N. parisii* and *N. ausubeli* during infection, we analysed RNA-seq results of each microsporidia species between *C. elegans* and *C. briggsae* at 10, 20, and 28 hours post infection. First, we used principal component analysis to compare microsporidia gene expression in each of these samples. We observed that at the 10-hour time point, there is a larger difference between expression in the two hosts, and at the later time points, expression in the two hosts is similar (figs. 3A and B). The 20- and 28-hour time points in *N. parisii* cluster closely together, but there is a larger difference between these time points in *N. ausubeli*, likely due to the accelerated growth of this species (Balla *et al.*, 2016). Moreover, we observed the expression of genes in each microsporidia species to be similar between the two *Caenorhabditis* hosts across the timepoints (figs. 3C and D, S1A and S1B). Strong correlation of *Nematocida* gene expression between *C. elegans* and *C. briggsae* was also observed, with similar levels of correlation of each microsporidia species in either host than between replicates in the same host (figs. 3E and F, S1C and S1D). These similarities between expression in different host species also did not change across time points as the parasite had gone through larger amounts of replication. At 10 hours post infection, over 45% of *Nematocida* genes are within 2-fold of each other, and over 60% are within four-fold of each other. As the time post infection increased to 28 hours, over 75% of *Nematocida* genes are within two-fold of each other, and more than 89% are within four-fold of each other. The similarity is even more pronounced in highly expressed genes (genes with greater than 100 FPKM in either host) at the 20- and 28-hour time point where 95-99% are within four-fold of each other.

To determine genes that are significantly differentially regulated depending upon the host species infected, we compared the 10-hour time points of each *Nematocida* species between the two hosts at 10 hours post infection (fig. 4A and B). We identified 34 differentially regulated genes in *N. parisii* and 11 in *N. ausubeli* ($\alpha < 0.05$) (Supplementary table S1). Most of these differentially regulated genes had higher expression in *C. elegans* than *C. briggsae* (31/34 in *N. parisii* and 7/11 in *N. ausubeli*). Notably, differentially regulated genes were significantly enriched for ribosomal protein genes in both *N. parisii* (17/34, Fisher's exact test p -value= 2.2×10^{-18}) and *N. ausubeli* (6/11, Fisher's exact test p -value= 1.2×10^{-8}). Taken together, our results indicate that the transcriptional programs of *N. parisii* and *N. ausubeli* are largely independent of which *Caenorhabditis* hosts they infect.

161
162
163
164
165
166
167
168
169
170
171
172
173
174
175
176
177
178
179
180
181
182
183
184
185
186
187
188
189
190
191
192
193
194
195
196
197
198
199
200
201
202
203
204
205
206
207
208
209
210
211
212
213
214
215

Shared and unique transcriptional responses of each *Caenorhabditis* host to *N. parisii* and *N. ausubeli* infection

Different microsporidia species may induce similar or distinct transcriptional responses in the same host. To address this question, we compared how either *C. elegans* or *C. briggsae* responded to infection with either *N. parisii* or *N. ausubeli* at the 10-hour timepoint for which we had replicate data. We first mapped the reads from each sample to the corresponding host genome (Supplementary table S2). In *C. elegans*, we identified 875 genes that are significantly differentially regulated in *N. parisii* infected samples and 735 genes that are significantly differentially regulated in *N. ausubeli* infected samples (fig. 5A-B and Supplementary table S3). For *C. briggsae*, 1091 genes are significant in *N. parisii* infected samples while 449 were significant in *N. ausubeli* infected samples (fig. 5C-D and Supplementary table S3). There are more downregulated than upregulated genes in each sample. Next, we directly compared shared genes which are upregulated in each of the *Caenorhabditis* hosts when infected by *N. parisii* or *N. ausubeli*. We observed significant overlap in the transcriptional response to these infections with 222 upregulated genes shared in *C. elegans* and 117 upregulated genes shared in *C. briggsae*.

We next compared both the overlapping and unique genes between samples to determine if they are enriched in known biological functions. Using statistical enrichment tests, we observed that the shared upregulated genes in *N. parisii* and *N. ausubeli* infected *C. elegans* are enriched for GO Biological Process associated with metabolism; as well as GO Molecular Process associated with catalytic activity (FDR<0.05, Supplementary table S4). We did not observe any enrichment in the shared upregulated genes in *C. briggsae*, however the 267 shared downregulated *C. briggsae* genes showed enrichment for small molecule binding and structural constituent of cuticle (Supplementary table S4). Of the non-shared genes, only the 415 downregulated genes in *C. briggsae* infected with *N. parisii* showed enrichment for GO Molecular Process associated with structural constituent of cuticle and protein binding (Supplementary table S4).

We then compared our RNA-seq data to previously published studies of the transcriptional response to *N. parisii* infection (Supplementary table S5). Bakowski *et al.* performed RNA-seq at multiple time points of a germline-deficient mutant of *C. elegans* continuously infected with spores at the L3/L4 stage at 25°C. We compared our 10-hour time point to the five time points in the Bakowski *et al.* study and observed strong overlap especially at the 8-, 16-, and 30-hour time points (Supplementary fig. S2A). We observed significant overlap for all the time points with both our *N. parisii* and *N. ausubeli* 10-hour post infection samples (fig. S2B-C). We also compared our data to Chen *et al.* where *C. elegans* was infected with *N. parisii* at the L3 stage at 20°C. We observed significant overlap with both our 10-hour *N. parisii* and *N. ausubeli* data (fig. S2D-E). Chen *et al.* also measured Orsay virus infected *C. elegans* and Santeuil virus infected *C. briggsae* and we saw significant similarities to these as well (fig. S2E-D). Together our analysis demonstrates that despite the experimental differences between studies, a largely similar upregulated host response is consistently observed.

Evolutionary conserved host response to *Nematocida* infection

To investigate the evolutionary conserved response of *Caenorhabditis* to *Nematocida* infection, we studied the expression levels of *C. elegans* and *C. briggsae* orthologs. We identified orthologs using Orthofinder (Emms and Kelly, 2019). Additionally, we determined the subset of orthologs that only had a single copy present in each nematode species. Of the orthogroups shared between *C. elegans* and *C. briggsae*, about 76% are single-copy orthologs (10826/14183). We first clustered the expression of these one-to-one orthologs, which shows a smaller cluster of upregulated genes and a larger cluster of downregulated genes (fig. 6A). When we compared the host response to infection between the two host species, we observed

216 a modest but significant correlation of response to infection between *C. elegans* and *C.*
217 *briggsae* (fig. 6B). We then compared the statistical significance to the fold change of
218 differentially expressed genes from the different infection conditions (fig. 6C-D) and
219 investigated which of these differentially expressed genes were one-to-one orthologs (fig. 6E-
220 F). We observed that only 8-17% of the differentially upregulated genes were one-to-one
221 orthologs. Furthermore, of the most highly expressed genes (greater than four-fold), only 0-2%
222 were one-to-one orthologs. In contrast to less than 20% of significantly upregulated genes not
223 having one-to-one orthologs, between 29-42% of significantly downregulated genes did.

224
225 As much of the upregulated response is in the non-single copy orthologs, we analysed these
226 genes for commonalities between samples. We performed domain enrichment analysis to
227 determine the types of proteins induced in the non-single copy orthologs by microsporidia
228 infection. Previous transcriptional analysis of *C. elegans* infected with either *N. parisii* or Orsay
229 virus has identified several types of domains enriched in expression, such as F-box,
230 MATH/BATH, PALS, DUF713, DUF684 and C-type lectins (Bakowski *et al.*, 2014; Chen *et al.*,
231 2017). In addition to these domains, we also included other types of domains that are enriched
232 in the significantly upregulated and downregulated non-single copy orthologs, for a total of
233 thirteen domains that we analysed (Supplementary table S6). Finally, the proportion of each
234 type of domain or gene family in the upregulated and downregulated non-single copy orthologs
235 was determined (fig. 7A-B). For *C. elegans* infected with *N. parisii*, we observed that ~29% of
236 the significantly expressed non-single copy orthologs contained at least one of these thirteen
237 domains, with genes containing PALS domains being the most common. For genes
238 upregulated after infection with *N. ausinger*, we observed similar trends with ~35% containing
239 one of these domains. The downregulated genes showed similar domain patterns for both
240 microsporidia species, with cuticle collagen and glycosyltransferase being the two most
241 common domains. Similar patterns regarding types of domains in regulated genes induced by
242 the two microsporidia species was also observed in *C. briggsae* (fig. 7B).

243
244 As some of the same expanded gene families are upregulated in both *C. elegans* and *C.*
245 *briggsae*, we sought to determine the relationships between expression of these families in
246 response to infection. We first constructed gene trees of PALS and DUF713 families (figs.
247 S3-S4). Next, we compared the expression levels of these orthologs in our 10-hour samples.
248 This analysis shows that some phylogenetically related PALS and DUF713 genes are
249 upregulated in both *C. elegans* and *C. briggsae* in response to *Nematocida* infection (fig. 8A-
250 B).

251 252 Discussion

253 To understand the conservation of transcriptional responses during microsporidia infection,
254 we took the approach of comparing interactions between related microsporidia and host
255 species. To do this we, used a pair of *Nematocida* species that share ~66% amino acid identity
256 and have distinct growth and phenotypic characteristics during infection in *C. elegans* (Cuomo
257 *et al.*, 2012; Balla *et al.*, 2016; Luallen *et al.*, 2016). We used a pair of *Caenorhabditis* species,
258 for which about 60% of their genes are orthologous and these proteins are 80% identical,
259 which is approximately the same extent of divergence between humans and mice (Stein *et al.*,
260 2003). We found that responses between *Caenorhabditis* and *Nematocida* species are largely
261 conserved. However, there are several limitations to our study. Although we monitored
262 infection at multiple time points, we only performed duplicates at 10 hours post infection.
263 Although a small number of replicates limit the ability to detect differentially regulated genes
264 (Conesa *et al.*, 2016), we saw a large overlap in significantly regulated genes compared to
265 other *N. parisii* infection datasets (Bakowski *et al.*, 2014; Chen *et al.*, 2017). Our study is also
266 limited to only two pairs of hosts and microsporidia species. Additionally, differences in
267 transcriptional responses between species could be dependent upon particular host and
268 microsporidia strains or environmental conditions.

269

270 Our results suggest that *Nematocida* microsporidia species do not sense and respond
271 differently depending upon their host environment. The main difference we observed in
272 *Nematocida* gene expression between the two hosts was an upregulation of both small and
273 large ribosomal subunit genes in *C. elegans* at 10 hours post infection. We also observed
274 about three-fold more ribosomal genes being differentially regulated between *N. parisii* and *N.*
275 *ausubeli*. After invasion both species undergo a lag period before starting replication. This lag
276 period is slightly shorter in *N. ausubeli* and the larger increase of ribosomal genes in *N. parisii*
277 is potentially related to these differences in lag time (Balla *et al.*, 2016). The lack of large
278 differences in the host response also suggests that these *Nematocida* microsporidia are not
279 differentially regulating host genes for their own benefit.

280
281 How hosts sense microsporidia infection is not fully understood. In mammals, several toll-like
282 receptors are necessary for immune activation (Tamim El Jarkass and Reinke, 2020), but the
283 proteins that *C. elegans* uses to sense and respond to microsporidia infection are mostly
284 unknown. Several negative regulators of the IPR are known, including PALS-22, LIN-35, and
285 PNP-1, but none of these are known to be necessary for the response to infection (Reddy *et*
286 *al.*, 2017, 2019; Tecele *et al.*, 2021; Willis *et al.*, 2021). Recently, a basic-region leucine-zipper
287 transcription factor, ZIP-1, was found to positively regulate a subset of IPR genes (Lažetić *et*
288 *al.*, 2022). A viral RNA receptor, DRH-1, is necessary for activation of the IPR by the Orsay
289 virus, but not for microsporidia infection (Sowa *et al.*, 2019). Whether there is an equivalent
290 protein that is specifically involved in detecting microsporidia infection in *C. elegans* is
291 unknown. Although a previous study showed that three IPR genes were induced to a lesser
292 extent by *N. ausubeli* than *N. parisii* (Zhang *et al.*, 2016) by comparing the full transcriptional
293 profile we see a largely similar set of genes being induced. As these different microsporidia
294 species induce a similar transcriptional response, this suggests that some common feature,
295 such as invasion, is detected by the host.

296
297 Nematodes, insects, and vertebrates all have strong transcriptional responses to infection by
298 microsporidia, though the responses appear to be quite diverse (Szumowski and Troemel,
299 2015; Middtun *et al.*, 2020). For example, antimicrobial peptides are observed to be
300 upregulated in silkworms and cytokines are induced in infected human cells (Ma *et al.*, 2013;
301 Flores *et al.*, 2021). The responses seen in these other animals are quite different than what
302 is observed in *Caenorhabditis*. One reason for this is that many IPR genes are part of large
303 gene families that are not conserved outside of *Caenorhabditis*, such as PALS (Leyva-Díaz *et*
304 *al.*, 2017). Little is known about how a host responds to different species of microsporidia. A
305 study examining two species of microsporidia that infect the same mosquito found that a
306 horizontally transmitted species elicited a strong transcriptional immune response, but this
307 response was not enriched during infection with a vertically transmitted species (Desjardins *et*
308 *al.*, 2015). Further studies will be necessary to know if the similar immune responses we
309 observe to infection by two horizontally transmitted microsporidia species are common in other
310 hosts infected by different microsporidia.

311
312 Microsporidia that infect free-living terrestrial nematodes appear to be common, and there are
313 other genera and families of nematodes that can be cultured in the laboratory and infected
314 with microsporidia. Additionally, there are other genera of microsporidia that have been shown
315 to infect *C. elegans* and other nematodes. Some nematode-infecting microsporidia also infect
316 multiple genera of nematodes, which could facilitate cross-species host expression (Zhang *et*
317 *al.*, 2016). These types of broader comparisons would allow for a fuller view of how animals
318 evolve transcriptional responses to microsporidia infection.

319 **Material and Methods**

320 **Infection of nematodes with microsporidia**

321
322
323

324 *C. elegans* strain N2 and *C. briggsae* strain AF16 were maintained at 21°C on 10-cm
325 nematode growth medium (NGM) plates seeded with *Escherichia coli* OP50-1 for at least three
326 generations without starvation. Three plates each of mixed stage populations of animals were
327 washed with M9 and embryos extracted by treating with sodium hypochlorite/1 M NaOH for
328 2.5 minutes. Embryos were hatched by incubating for 18 hours at 21°C. ~30,000 L1s of each
329 species were placed on a 10-cm plates along with 1 ml M9 and 10 µl of 10X OP50-1. Three
330 plates of each species were prepared. Animals were infected with either 20 million *N. parisii*
331 (ERTm1) or *N. ausubeli* (ERTm2) spores. These spores were prepared as described
332 previously (Troemel *et al.*, 2008). Uninfected plates were used as the control. Plates were
333 dried for 1 hour in a clean cabinet and incubated an additional 1.5 hours at 21°C. Animals
334 were then removed from plates using two 5 ml washes of M9. After washing samples twice
335 with 10 ml M9, all but 1 ml of M9 was removed from the samples. An additional 3 ml of M9
336 and 1 ml of 10X OP50-1 was added to each sample, and 1 ml of this solution was plated onto
337 4 10-cm plates per sample, resulting in ~6,000 animals per plate. At either 10, 20, or 28 hours
338 post infection, plates were harvested by washing off worms 3 times with 725 µl M9. Samples
339 were then washed 3 times with 1 ml M9/0.1% Tween-20.

340

341 To determine the extent of infection, ~1,000 animals from each sample were removed, fixed,
342 and stained using an *N. parisii* 18S rRNA fluorescent in situ hybridization probe as previously
343 described (Reinke *et al.*, 2017). Vectashield containing DAPI (Vector Labs) was added and
344 samples imaged using an Zeiss Axioimager 2.

345

346 **RNA extraction and sequencing**

347 After the last wash, 1 ml of TRIzol was added to each sample and RNA was extracted similar
348 to as described previously (Bakowski *et al.*, 2014). mRNA libraries were prepared by the
349 UCSD IGM Genomics Center and sequenced on a single lane of an Illumina HiSeq 4000,
350 using 100 bp paired-end reads.

351

352 **Microsporidia gene expression analysis**

353 Reads from each sample were mapped to either *Nematocida parisii* strain ERTm1 (Genbank:
354 GCF_000250985.1) or *Nematocida ausubeli* strain ERTm2 (Genbank: GCA_000250695.1)
355 using TopHat v2.1.2 (Trapnell, Pachter and Salzberg, 2009). The respective *N. parisii* and *N.*
356 *ausubeli* genome annotation files were converted into .gtf format using Gffread v0.12.3.
357 Transcriptome assemblies were then generated using Cufflinks v2.2.1 (Trapnell *et al.*, 2010)
358 and Cuffmerge in the Cufflinks package. Differentially expressed genes were determined
359 using Cuffdiff v2.2.1 (Trapnell *et al.*, 2013) and were visualised using the R package
360 cummeRbund v2.36.0 (L. Goff, 2017).

361

362 The Fragments Per Kilobase of transcript per Million mapped reads (FPKM) values of *N. parisii*
363 and *N. ausubeli* transcripts in each *Caenorhabditis* host were calculated by Cuffdiff v2.2.1
364 (Trapnell *et al.*, 2013). The linear correlation between gene expression in each host was
365 determined using the R packages ggplot2 v3.3.5 and ggpubr v0.4.0; the ratio of FPKM values
366 between the two hosts was calculated by dividing the microsporidia's FPKM values in *C.*
367 *elegans* by that of *C. briggsae*'s. Hierarchical clustering of log₁₀-transformed FPKM+1 values
368 was done using the hclust function from the R package stats v4.1.1; heatmaps were generated
369 by ggplot2 v3.3.5 in R.

370

371 ***Caenorhabditis* RNA-seq analysis**

372 The paired end reads of each sample 10 hours post infection sample were submitted to Alaska
373 v1.7.2 (<http://alaska.caltech.edu>). Briefly, Bowtie2 (Langmead and Salzberg, 2012), Samtools
374 (Li *et al.*, 2009), RSeQC (Wang, Wang and Li, 2012), FastQC, and MultiQC (Ewels *et al.*, 2016)
375 were used for quality control of the input files. Then, Kallisto (Bray *et al.*, 2016) was used for
376 read alignment and quantification, followed by differential analysis using Sleuth (Pimentel *et*
377 *al.*, 2017). For *C. elegans* samples, the reads were aligned to the N2 reference of the WS268

378 release (accession: PRJNA13758); the reads from *C. briggsae* samples were aligned to
379 reference genome of the WS268 release (accession: PRJNA10731).

380

381 Log2 fold change values of duplicated genes in each of the eight samples were averaged
382 using the R package dplyr v1.0.8. Genes with FDR-adjusted p-value of <0.05 were regarded
383 as significant. Differentially upregulated genes were defined as those with an FDR-adjusted
384 p-value<0.05 and log2 fold change ≥ 0 (infected vs. control); differentially downregulated
385 genes were defined as those with an FDR-adjusted p-value <0.05 and log2 fold change ≤ 0
386 (infected vs. control).

387

388 **Principal component analysis**

389 The normalised abundance measurements in *C. elegans* and *C. briggsae* generated by Alaska,
390 were read by the readRDS() function of the R package base v4.1.1. Normalized counts for
391 each gene in each host species were generated via sleuth_to_matrix() with the “obs_norm”
392 data and “tpm” units. PCA of gene expression was performed using samples from each
393 species via the R package pcaexplorer v2.20.2 (Marini and Binder, 2019).

394

395 **Determination of gene expression overlap**

396 Genes with an FDR<0.05 were used to compare expression overlap. Values of duplicated
397 genes in each sample were averaged using the R package dplyr v1.0.8. Overlap between
398 samples was determined using the R package gplots v3.1.1. The p-values were calculated
399 using the Fisher exact test. Statistical enrichment tests of shared and non-shared genes were
400 performed using PANTHER on pantherdb.org (Mi *et al.*, 2021). Each input list was statistically
401 tested for enrichment against the annotation sets: “GO biological process complete”, “GO
402 cellular component complete”, “GO molecular function complete”, “PANTHER GO-Slim
403 Biological Process”, “PANTHER GO-Slim Cellular Component”, “PANTHER GO-Slim
404 Molecular Function”, “PANTHER Pathways”, “Reactome pathways” and “PANTHER Protein
405 Class”. Results from these tests with p-value<0.05 are in Supplementary table S4.

406

407 To determine overlap in our samples compared to differentially regulated genes from
408 Bakowski *et al.*, we first used Alaska to process the read files of *C. elegans* infected by *N.*
409 *parisii* samples at 8, 16, 30, 40 and 64 hours. To compare our samples’ expression with data
410 from Bakowski *et al.*, genes expressed in at least four of those samples were used for
411 hierarchical clustering by hclust function in the R package stats v4.1.1. The dendrogram in the
412 was produced using the R package gg dendrogram v0.1.23; the heatmap was generated by
413 ggplot2 v3.3.5. Overlap between our samples, the Bakowski *et al.*, (2014) samples, and the
414 Chen *et al.* (2017) samples containing differentially regulated genes for *C. elegans* N2 infected
415 by Orsay virus or *N. parisii*, and *C. briggsae* infected by Santeuil virus were calculated as
416 described above.

417

418 **Domain enrichment analysis**

419 The type of gene classes and domains investigated for the enrichment analyses are listed in
420 Supplementary table S6. Among these, we actively chose to look at F-box, MATH/BATH,
421 PALS, DUF684, DUF713, C-type lectins, and *skr* domains containing genes, implicated from
422 differentially regulated genes of *N. parisii* infected *C. elegans* in previous publications
423 (Bakowski *et al.*, 2014; Chen *et al.*, 2017). We also examined additional types of genes and
424 domains enriched in our datasets using DAVID Bioinformatics Resources (2021) (Huang, Brad
425 T. Sherman and Lempicki, 2009; Huang, Brad T Sherman and Lempicki, 2009) for *C. elegans*
426 and the WormBase Simple Gene Queries tool for *C. briggsae*. From this analysis, we found
427 additional domains and genes enriched with greater than three domain-containing proteins in
428 any of our samples. These identified domains are chitinase-like (*chil*) proteins, CUB and CUB-
429 like domains, cytochrome P450, glucosyltransferase family 92, nematode cuticle collagen N-
430 terminal domain, and UDP-glucuronosyltransferase. A list of gene names from respective
431 gene classes were downloaded separately from Wormbase (<http://wormbase.org/>) and the
432 corresponding protein-coding sequences were extracted from Wormbase ParaSite

433 (<https://parasite.wormbase.org/>). Alignments of other domains or classes were downloaded
434 directly from Pfam (<http://pfam.xfam.org/>) separately. After deleting duplicated sequences,
435 protein sequences of these classes of genes were converted to Stockholm format using
436 Clustal Omega Multiple Sequence Alignment tool (<https://www.ebi.ac.uk/Tools/msa/clustalo/>).
437 Hmmbuild of HMMER v3.3.2 (Eddy, 2011) was used to build respective profile HMMs, which
438 was then searched against *C. elegans* (accession: PRJNA13758) proteome of WS268 release
439 using hmmsearch. Output genes with E-value <1e-5 were used as the gene list for the
440 enrichment analyses. In the output genes, MATH and BATH genes were combined into one
441 list; *fbxa*, *fbxb* and *fbxc* genes were merged into the gene list for F-box while genes with CUB
442 and CUB-like domains were categorised together (Supplementary table S6). Using the R
443 package gplots v3.1.1, the number of genes overlapping between the lists and samples were
444 computed, then plotted using R package ggplot2 v3.3.5. Genes that do not fall into any of
445 these gene classes or have any of these domains were categorized as “other”.

446 **Determination of orthologs between *C. elegans* and *C. briggsae***

447 Orthologous genes were determined between *C. elegans* (accession: PRJNA13758) and *C.*
448 *briggsae* (accession: PRJNA13758) proteomes of the WS268 release using Orthofinder v2.5.2
449 with the default settings (Emms and Kelly, 2019).

451 **Single copy orthologs analysis**

452 Genes that are single copy orthologs were extracted, based on the single copy orthologs list
453 computed by Orthofinder. Single copy orthologs expressed in at least one out of the four
454 samples were used for hierarchical clustering via the function hclust() from the R package
455 stats v4.1.1, then plotted using R packages gg dendrogram and ggplot2 v3.3.5. The linear
456 correlation of each single copy ortholog expression between the two host was calculated using
457 ggpubr v0.4.0. The scatterplots and volcano plots were generated by ggplot2 v3.3.5.

459 **Comparison of gene expression in expanded gene families**

460 The *C. elegans* and *C. briggsae* genes in PALS and DUF713 families were obtained from the
461 output of HMMER v3.3.2 (Eddy, 2011) using a E-value threshold of <1e-5. The protein
462 sequences of the genes were obtained from Wormbase ParaSite
463 (<https://parasite.wormbase.org/>) and aligned by M-Coffee using default settings (Notredame,
464 Higgins and Heringa, 2000; Di Tommaso *et al.*, 2011). A phylogenetic tree for each family was
465 generated using MrBayes (Huelsenbeck and Ronquist, 2001; Ronquist and Huelsenbeck,
466 2003) with the following settings: lset nst = 1, rates = invgamma, nruns = 2, stoprule = YES,
467 stopval = 0.05 and mcmc diagn = YES. A dendrogram of the phylogenetic tree of each gene
468 family was created using the function ReadDendrogram from the R package DECIPHER
469 v2.22.0. For each gene family, the orthologs' log₂ fold change values across the *C. elegans*
470 and *C. briggsae* samples were plotted as a heatmap using ggplot2 v3.3.5.

472 **Data availability**

473 All samples were deposited under NCBI BioProject PRJNA841614 and the sequence reads
474 for all samples were submitted to the NCBI Sequence Read Archive.

476 **Acknowledgements**

477 We thank Hala Tamim El Jarkass, Meng A. Xiao, and Winnie Zhao for providing helpful
478 comments on the manuscript. We thank Winnie Zhao for technical help for the comparisons
479 to the Bakowski data. This work was supported by a Canadian Institutes of Health Research
480 grant no. 400784 (to A.R.), an Alfred P. Sloan Research Fellowship FG2019-12040 (to A.R.),
481 and NIH R01's AG052622 and GM114139 to E.T. Some strains were provided by the CGC,
482 which is funded by NIH Office of Research Infrastructure Programs (P40 OD010440) and we
483 thank WormBase.

484

486 **Author contributions:** Y.C.W. and A.R. conceived of the project. Y.C.W. performed all
487 computational analyses. A. R. performed all experiments. E.T. and A. R. provided mentorship
488 and acquisition of funding. Y.C.W. and A.R. co-wrote the paper with edits from E.T.

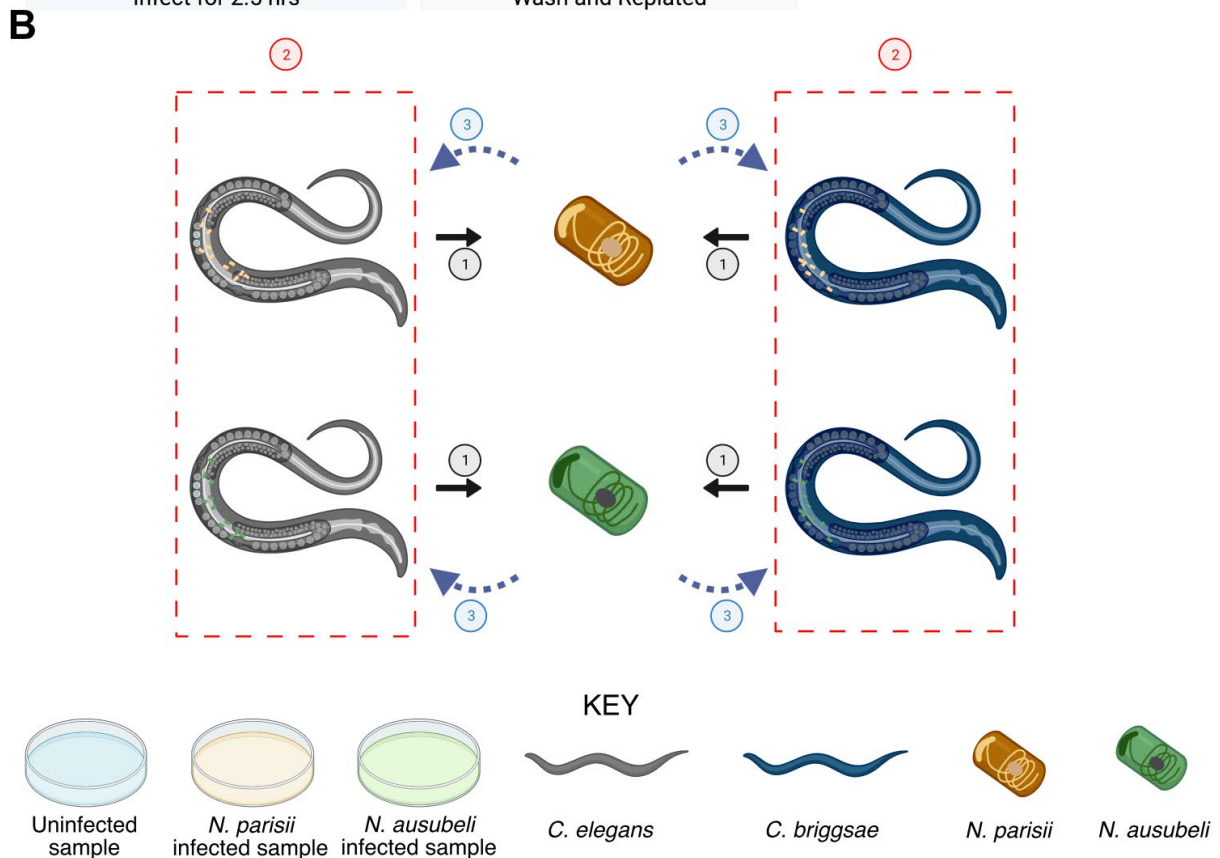
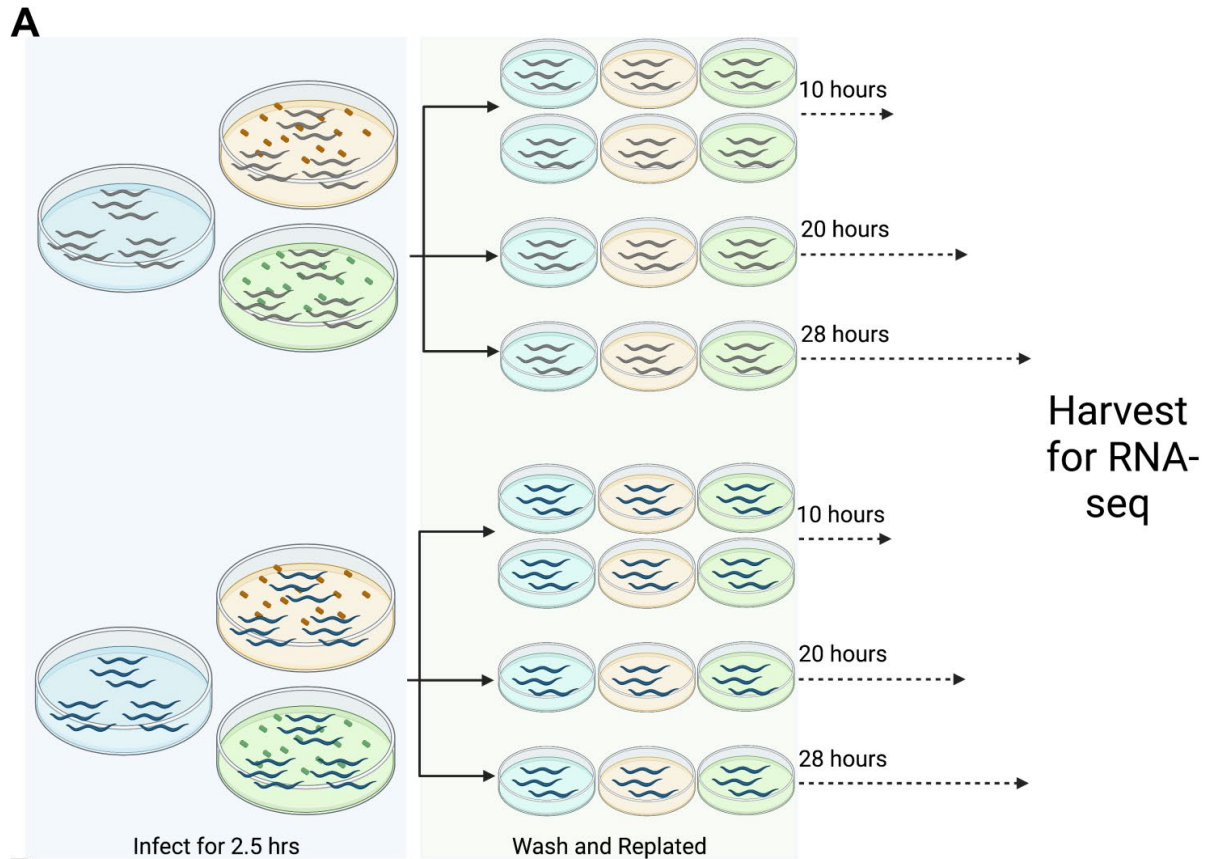
489

490 **Competing Interests:** The authors declare that they have no competing interests.

491

492 **Figures and legends**

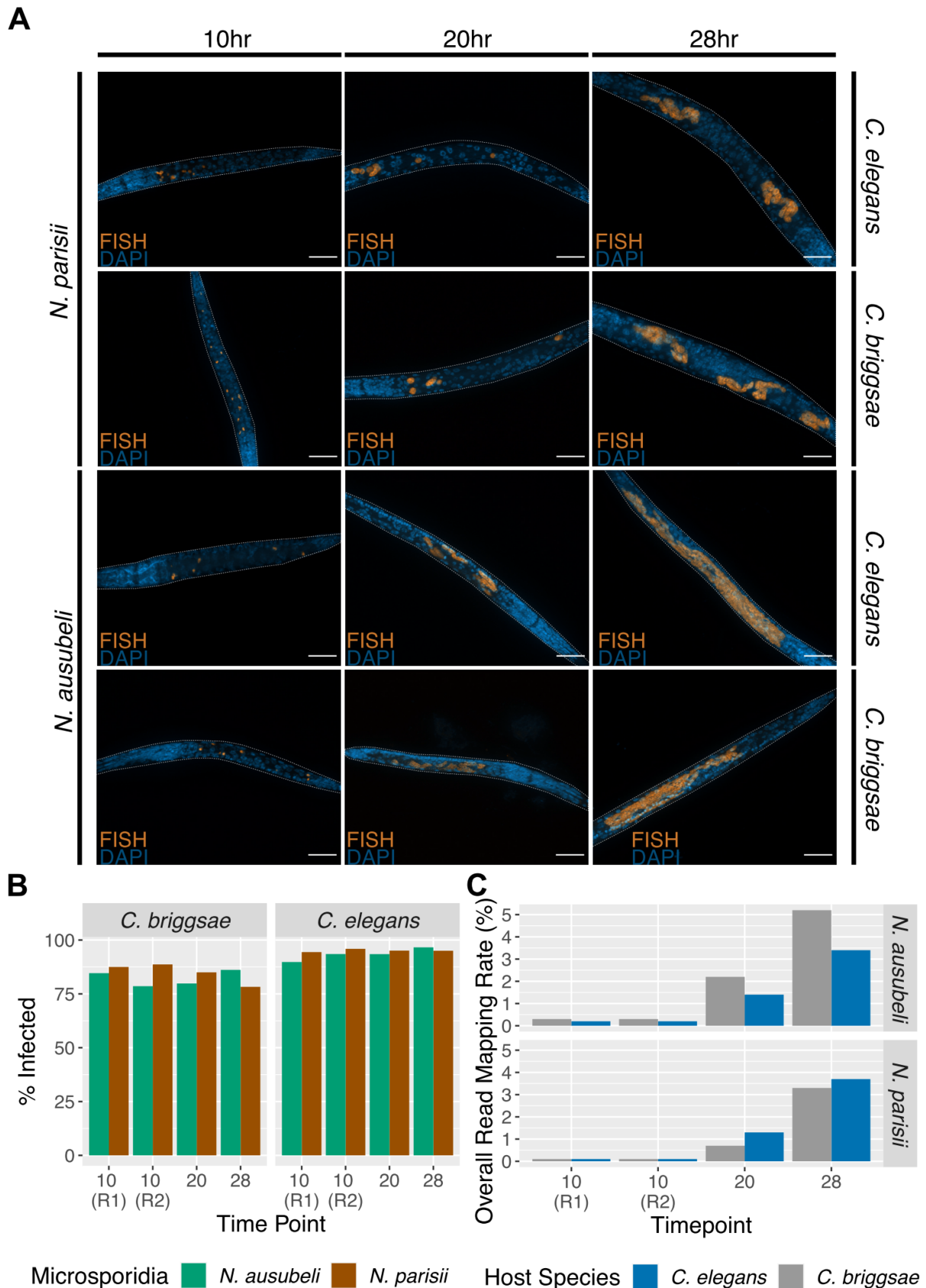
493



494
495
496
497
498

Fig. 1. Overview of study design. (A) Schematic diagram of the RNA-seq experiment. *C. elegans* and *C. briggsae* were either not infected or infected with *N. parisii* or *N. ausubeli* separately at the L1 stage for two and a half hours. Next, animals were washed to remove any remaining microsporidia spores and replated. Worms were harvested for RNA-sequencing at

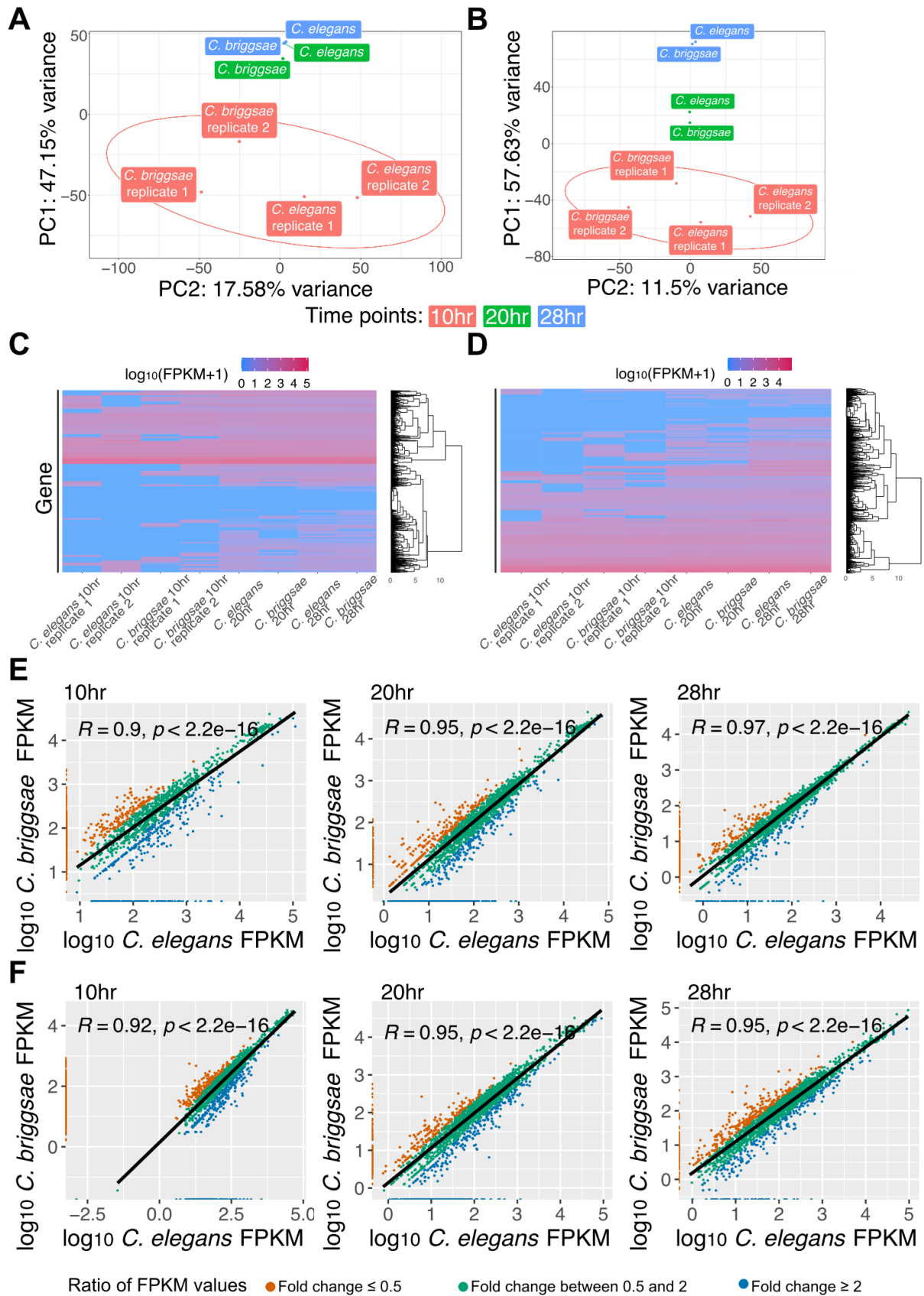
499 10, 20 and 28 hours after infection. (B) The three comparisons of transcriptional responses
500 made in this study are represented. Comparison 1 is microsporidia gene expression between
501 hosts, comparison 2 is the response of each host species to different microsporidia species,
502 and comparison 3 is the conserved response between different hosts to each microsporidia
503 species. Figure was created with biorender (www.biorender.com).
504



505
506
507
508
509

Fig. 2. Nematocida infection of Caenorhabditis hosts. (A) Pulse-infected *C. elegans* or *C. briggsae* were fixed and then stained with DAPI to detect nuclei and a FISH probe specific to *Nematocida* 18S rRNA to detect either *N. parisi* or *N. ausubeli* at 10, 20 and 28 hours after

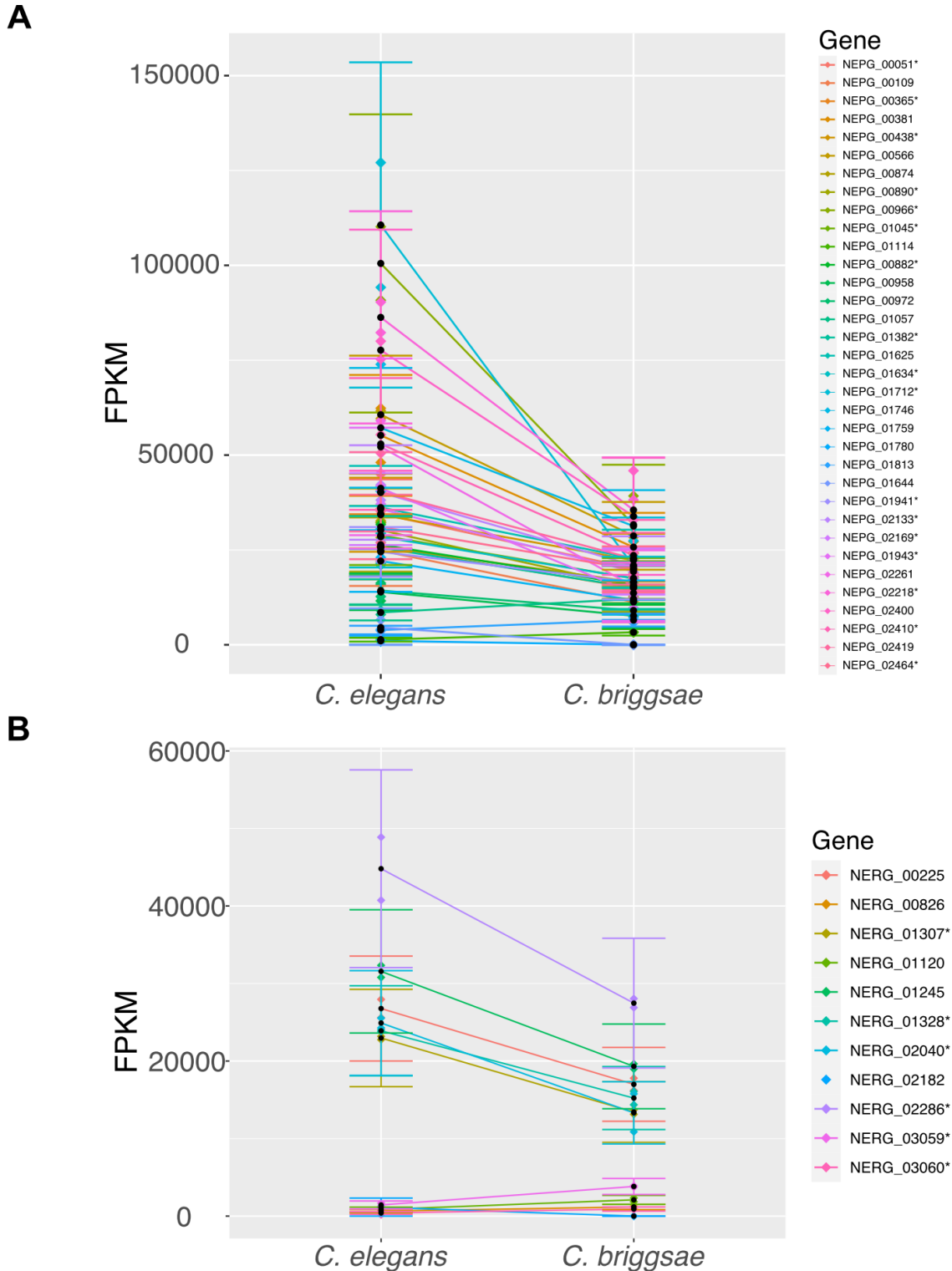
510 infection. Representative images of infection are shown. Scale bars are 23 μm . (B) Percentage
511 of infected animals at different timepoints. Between 39 to 220 animals were counted for each
512 sample. (C) Overall read mapping rate of *Nematocida* in each host at different time points. R1
513 or R2 indicates the replicate samples at the 10-hour timepoint.
514



515
516
517
518
519

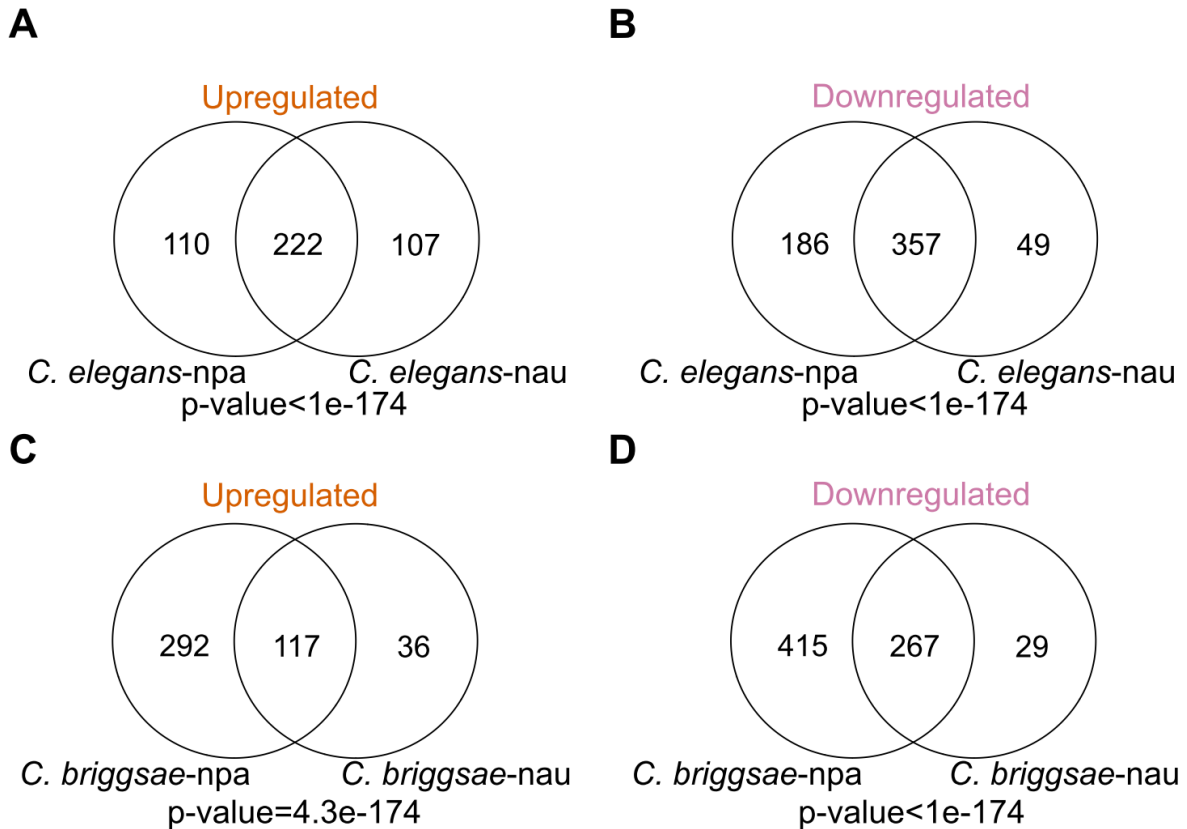
Fig. 3. Microsporidia gene expression in different host species. Principal component analysis of (A) *N. parisii* and (B) *N. ausubeli* in *C. elegans* and *C. briggsae* at 10, 20 and 28 hours. Circles represent confidence ellipses around each strain at 95% confidence interval.

520 (C-D) Heatmap of transcriptional profiles of genes expressed in *N. parisii* (C) and *N. ausubeli*
521 (D). Rows represent gene clustered hierarchically. Scale is of differential regulation of infected
522 compared to uninfected samples. (E-F) Scatterplot of log₁₀ FPKM values in *N. parisii* (E) and
523 *N. ausubeli* (F) when infecting *C. briggsae* and *C. elegans*. Each point represents a
524 microsporidian gene. Pearson correlation value and p-value are indicated on the top left of
525 each plot. The ratio of FPKM values for each gene between *C. elegans* and *C. briggsae* is
526 demonstrated by the colour of the points, which is described in the legend at the bottom.
527
528

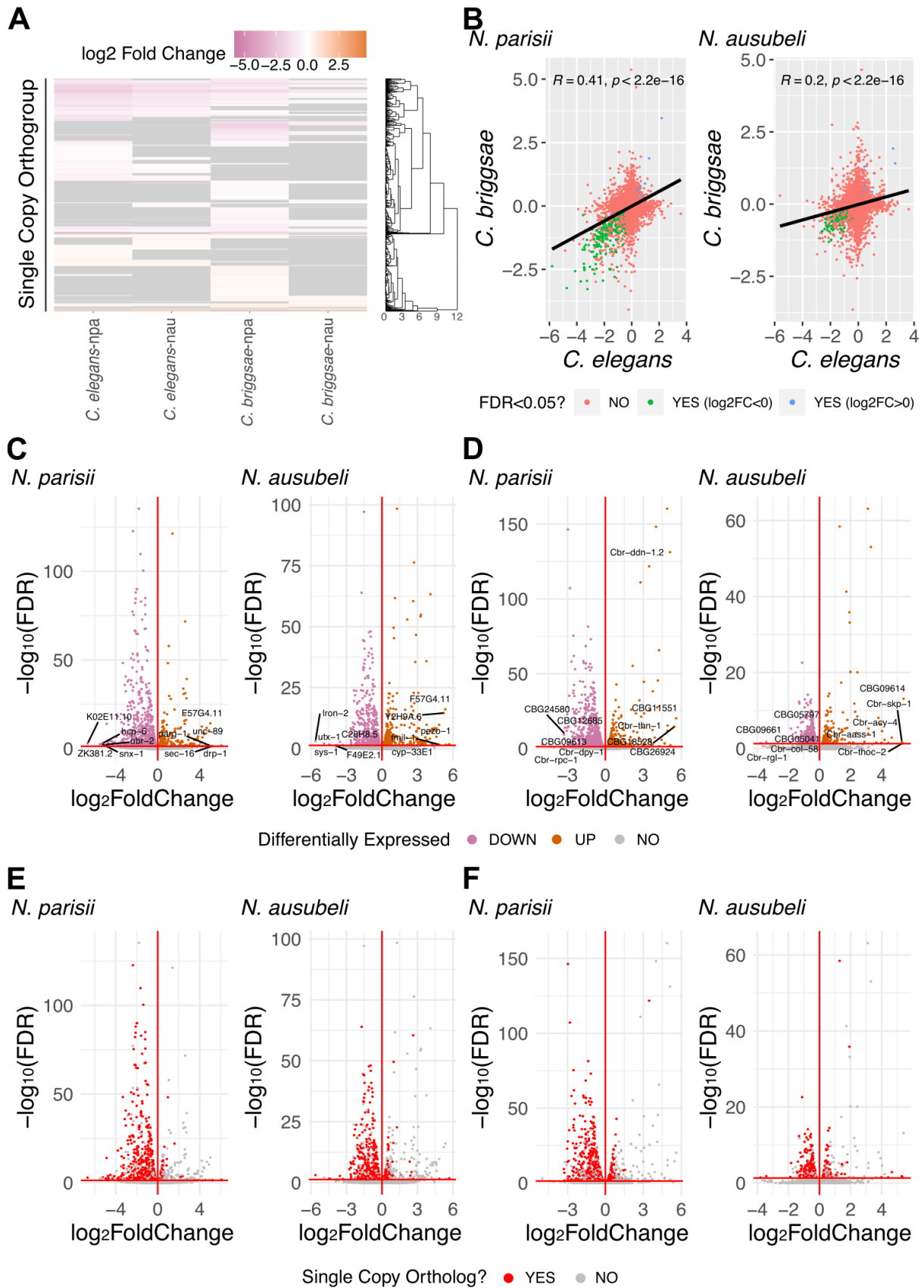


529

530 **Fig. 4. Differentially regulated genes of microsporidia.** (A-B) Line plots of the FPKM values
531 with confidence intervals, calculated for the differentially regulated genes (FDR<0.05) in *N.*
532 *parisii* (A) and *N. ausubeli* (B) at 10 hours post infection. * indicates ribosomal protein-
533 encoding genes. The aggregate sample value of the two replicates is noted as a black dot
534 within the confidence interval, while the value for each replicate is shown as a dot of matching
535 colour along the confidence interval. Error bars of each gene show the variability of the
536 distribution of FPKM values.
537
538



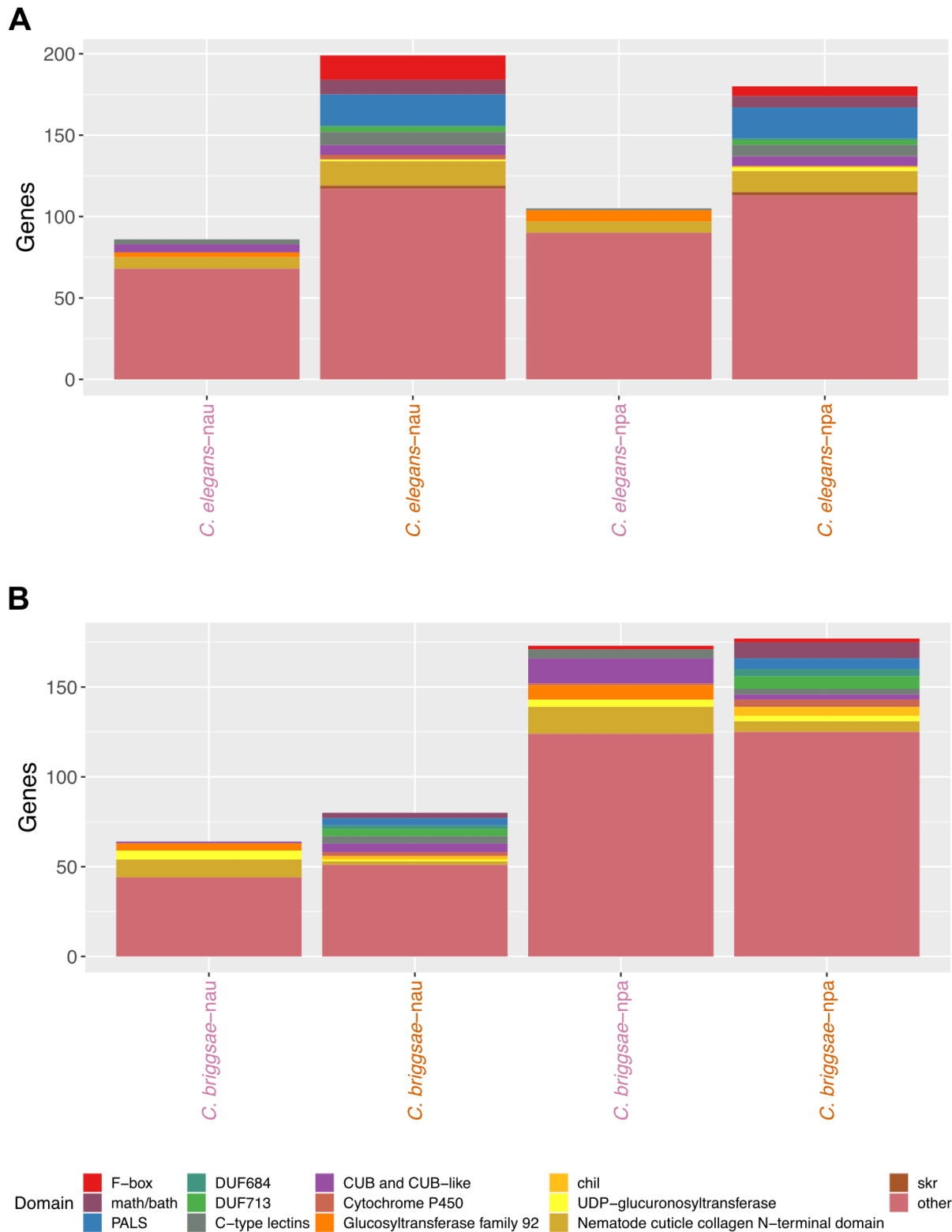
539
540
541 **Fig. 5. Transcriptional responses of *Caenorhabditis* hosts to *Nematocida* infection.** (A-
542 D) Venn diagrams of genes in *C. elegans* (A-B) or *C. briggsae* (C-D) that are upregulated (A
543 and C) or downregulated (B and D) when infected by *N. parisii* or *N. ausubeli*. npa (*N. parisii*)
544 and nau (*N. ausubeli*).
545
546



547
548
549
550
551

Fig. 6. Transcriptional responses of single copy orthologs in *Caenorhabditis* hosts to *Nematocida* infection. (A) Heatmap of transcriptional profiles of single-copy orthologs in *C. elegans* and *C. briggsae* after infection by *N. parisii* or *N. ausubeli*. Rows represent genes clustered hierarchically. Scale is of differential regulation of infected compared to uninfected

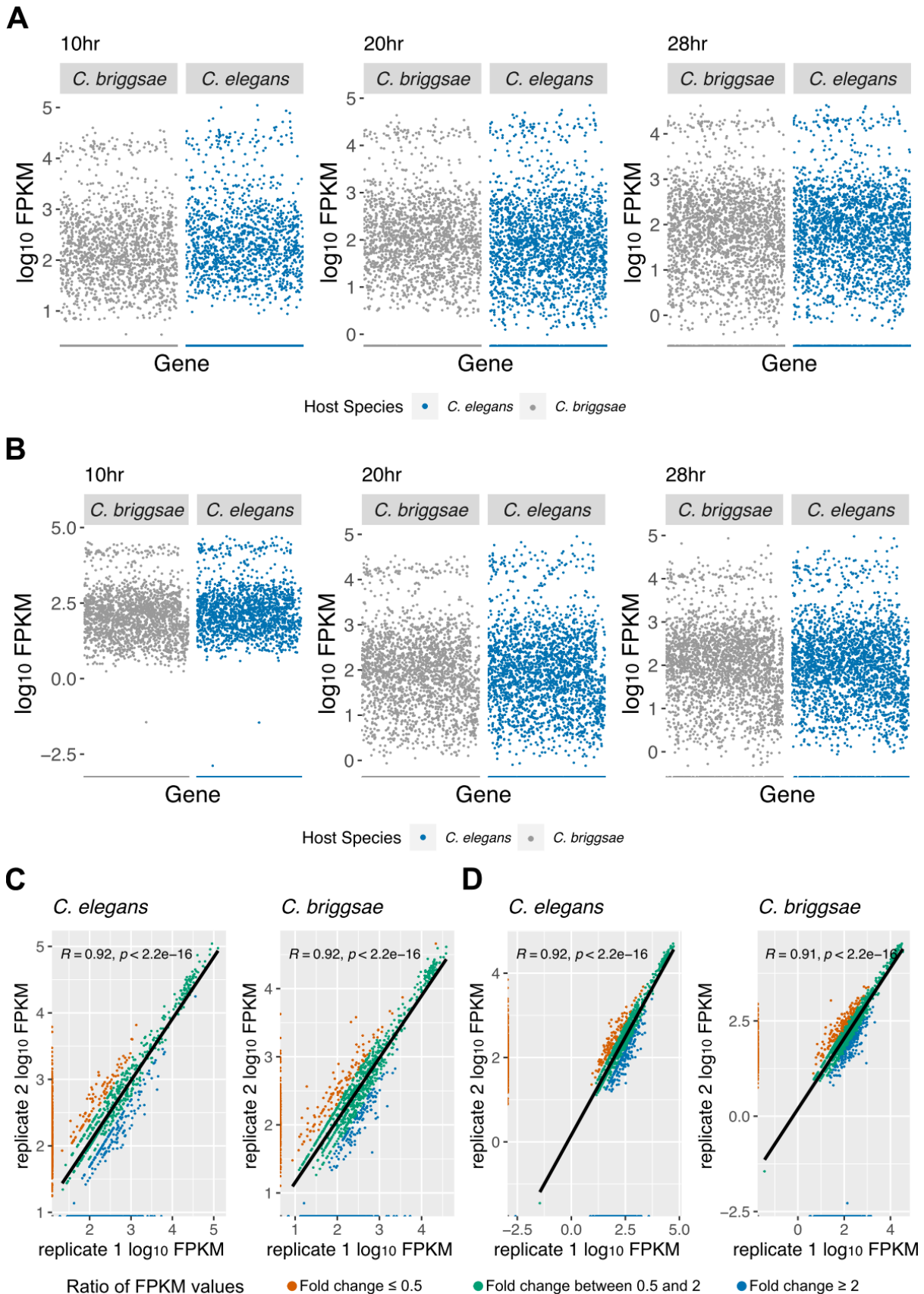
552 samples. **(B)** Scatterplot of log₂ fold change values of single-copy orthologs expressed in *C.*
553 *elegans* and *C. briggsae*. Each point represents a single-copy ortholog between the two host
554 species. Pearson correlation values and p-values are indicated on top left of each plot. The
555 ratio of log₂ fold change values for each single copy ortholog between *C. elegans* and *C.*
556 *briggsae* is demonstrated by the colour of the points. (C-D) Volcano plots of genes expressed
557 in *Nematocida* infected *C. elegans* (C) and *C. briggsae* (D). Upregulated genes are
558 represented with orange points; downregulated genes are represented with pink points. The
559 top 5 upregulated and downregulated genes are labelled. (E-F) Volcano plots of genes
560 expressed in *Nematocida* infected *C. elegans* (E) and *C. briggsae* (F). Single-copy orthologs
561 are represented with red points and non-single copy orthologs represented with grey points.
562 npa (*N. parisii*) and nau (*N. ausubeli*).
563
564



565
566
567
568
569
570
571

Fig. 7. Transcriptional responses of non-single copy orthologs in *Caenorhabditis* hosts to *Nematocida* infection. Domain enrichment analysis of significantly upregulated and downregulated non-single copy ortholog genes in *C. elegans* (A) and *C. briggsae* (B). npa (*N. parisii*) and nau (*N. ausubeli*). Upregulated samples are represented with orange text; downregulated samples are represented with pink text.

579



580

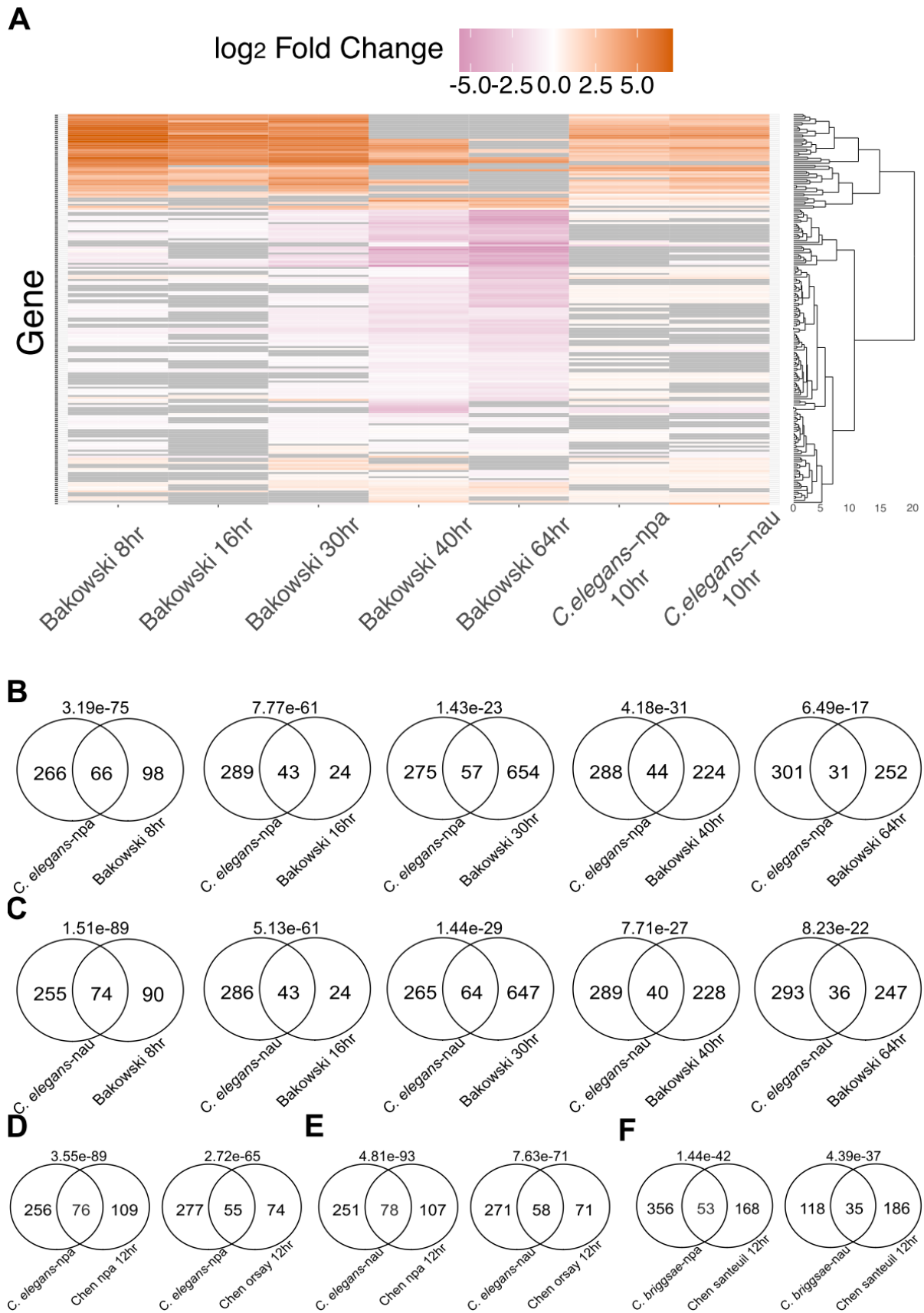
581

582

583

Fig. S1. Transcriptional response of *Nematocida* species in *Caenorhabditis* hosts. (A-B) Scatterplot of *N. parisii* (A) and *N. ausubeli* (B) log₁₀ FPKM values between *C. briggsae* and *C. elegans* replicates at 10 hours. Pearson correlation values and p-values are indicated

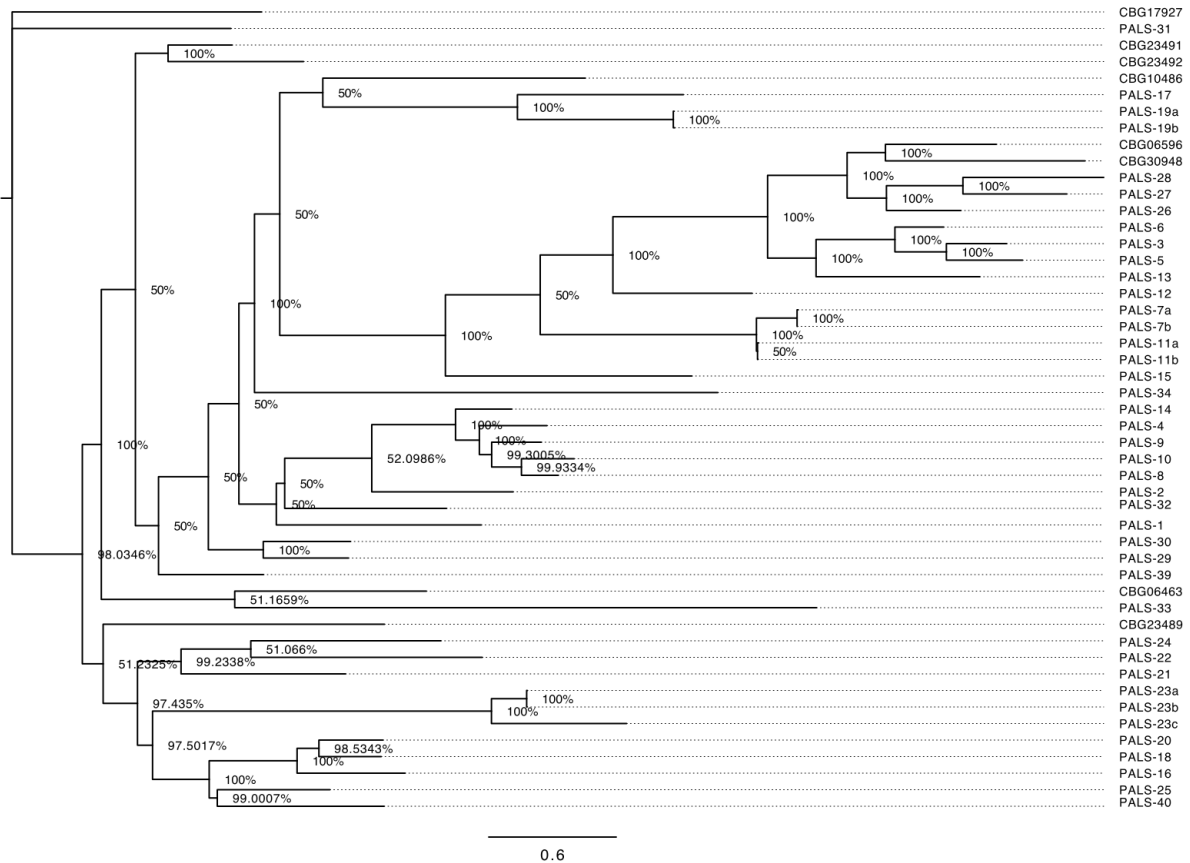
584 on the top left of each plot. The ratio of FPKM values for each gene between the replicates is
585 demonstrated by the colour of the points. (C-D) Gene expression pattern of *N. parisii* (C) and
586 *N. ausubeli* (D) in *C. elegans* and *C. briggsae*.
587
588



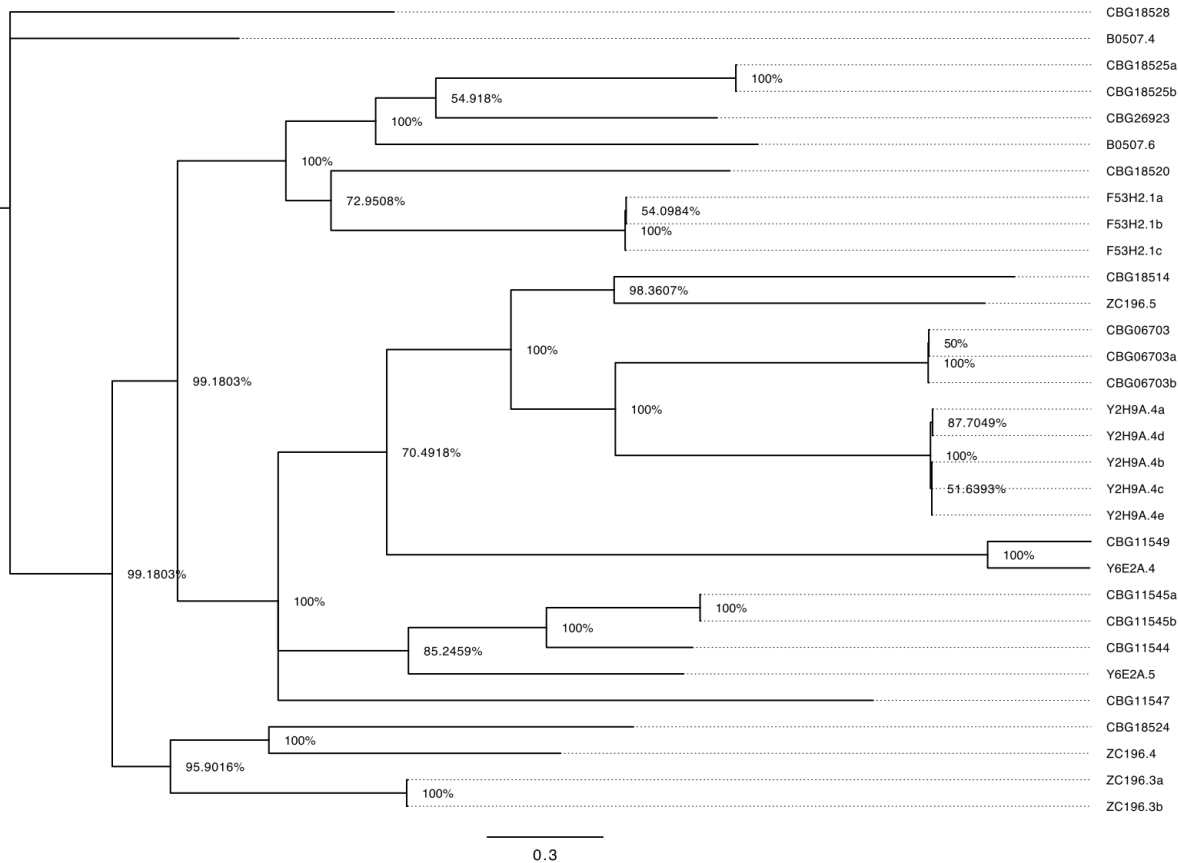
589
590
591
592
593

Fig. S2. Data from this study has high overlap with previously published intracellular infection samples. (A) Heatmap of transcriptional profiles of differentially regulated genes (FDR<0.05) across five samples from Bakowski *et al.* and our 10hr *N. parisii* and *N. ausubeli* infected *C. elegans* samples. Only genes expressed in at least four out of the eight total

594 samples are included. (B-C) Statistical overlap of significant genes between respective *N.*
595 *parisii* or *N. ausinger* infected *C. elegans* samples and Bakowski *et al.* samples across five
596 timepoints. (D-E) Statistical overlap of significant genes between *N. parisii* (D) or *N. ausinger*
597 (E) infected *C. elegans* samples and Chen *et al.* Orsay virus infected *C. elegans* sample at 12
598 hours. (F) Statistical overlap of significant genes between respective *N. parisii* or *N. ausinger*
599 infected *C. briggsae* sample and Chen *et al.* Santeuil virus infected *C. briggsae* sample at 12
600 hours. The p-value of each comparison is indicated on top of each Venn diagram. npa (*N.*
601 *parisii*) and nau (*N. ausinger*).
602
603



604
605 **Fig. S3. Phylogram of *C. elegans* and *C. briggsae* PALS family genes.** Genes with the
606 same name that end with different letters indicate protein isoforms. Node values indicate
607 posterior probabilities for each split as percentage. The scale bar indicates average branch
608 length measured in expected substitutions per site.
609
610



611
 612 **Fig. S4. Phylogram of *C. elegans* and *C. briggsae* DUF713 family genes.** Genes with the
 613 same name that end with different letters indicate protein isoforms. Node values indicate
 614 posterior probabilities for each split as percentage. The scale bar indicates average branch
 615 length measured in expected substitutions per site.

616
 617
 618
 619
 620

621 **Supplementary Table and Materials**

622 **Supplementary Table S1. FPKM values of gene expression and differentially expressed**
 623 **microsporidia genes.**

624
 625 **Supplementary Table S2. Normalised RNA-seq counts of the *C. elegans* and *C. briggsae***
 626 **for the transcriptional analysis generated by Alaska.**

627
 628
 629 **Supplementary Table S3. Differentially expressed genes of *C. elegans* and *C. briggsae***
 630 **exposed to the two species of microsporidia generated by Alaska.**

631
 632 **Supplementary Table S4. PANTHER GO enrichment analyses.** Sheet S1 contains results
 633 of the statistical enrichment tests of the 222 significantly upregulated genes shared between
 634 *N. parisii* and *N. ausinger* infected *C. elegans*. Sheet S2 contains results of the statistical
 635 enrichment tests of the 267 significantly downregulated genes shared between *N. parisii* and
 636 *N. ausinger* infected *C. briggsae*. Sheet S3 contains results of the statistical enrichment tests
 637 of the 415 significantly downregulated genes specifically in *N. parisii* infected *C. briggsae*.

638
 639 **Supplementary Table S5. List of gene set overlaps with previously published infection**
 640 **samples.**

641
642
643
644

Supplementary Table S6. Gene classes and domains used for enrichment analyses.

Domain/ Gene Family	Databse	Wormbase gene class OR Pfam ID
F-box	Wormbase	fbxa, fbxb, fbxc
MATH (mepirin or Traf homology) or BATH (BTB and MATH domain-containing)	Wormbase	math, bath
PALS (protein containing ALS2CR12 signature)	Wormbase	pals
C-type lectins	Wormbase	clcc
DUF713	Pfam	PF015218
DUF684	Pfam	PF05075
chil	Wormbase	chil
Nematode cuticle collagen N-terminal domain	Pfam	PF01484
CUB and CUB-like	Pfam	PF00431, PF02408
Cytochrome P450	Wormbase	cyp
Glucosyltransferase family 92	Pfam	PF00201
UDP-glucuronosyltransferase	Wormbase	ugt
skr (Skr1-related)	Wormbase	Skr
Other (Any genes not in the domain or gene family above)	-	-

645

References

646

647 Bakowski, M.A. *et al.* (2014) 'Ubiquitin-Mediated Response to Microsporidia and Virus
648 Infection in *C. elegans*', *PLoS Pathogens*. Edited by D.S. Schneider, 10(6), p. e1004200.
649 doi:10.1371/journal.ppat.1004200.

650

651 Balla, K.M. *et al.* (2016) 'Cell-to-cell spread of microsporidia causes *Caenorhabditis elegans*
652 organs to form syncytia', *Nature Microbiology*, 1(11), p. 16144.
doi:10.1038/nmicrobiol.2016.144.

653

654 Barrière, A. and Félix, M.-A. (2005) 'High Local Genetic Diversity and Low Outcrossing Rate in
655 *Caenorhabditis elegans* Natural Populations', *Current Biology*, 15(13), pp. 1176–1184.
doi:10.1016/j.cub.2005.06.022.

656

657 Bojko, J. *et al.* (2022) 'Microsporidia: a new taxonomic, evolutionary, and ecological
synthesis', *Trends in Parasitology*, 0(0). doi:10.1016/j.pt.2022.05.007.

658

659 Bray, N.L. *et al.* (2016) 'Near-optimal probabilistic RNA-seq quantification', *Nature
Biotechnology*, 34(5), pp. 525–527. doi:10.1038/nbt.3519.

660

661 Burton, N.O. *et al.* (2021) 'Intergenerational adaptations to stress are evolutionarily
662 conserved, stress-specific, and have deleterious trade-offs.', *eLife*, 10.
doi:10.7554/eLife.73425.

663

664 Chen, K. *et al.* (2017) 'An evolutionarily conserved transcriptional response to viral infection
665 in *Caenorhabditis nematodes*', *BMC Genomics*, 18(1), p. 303. doi:10.1186/s12864-017-3689-
3.

- 666 Conesa, A. *et al.* (2016) 'A survey of best practices for RNA-seq data analysis', *Genome*
667 *Biology*, 17(1), p. 13. doi:10.1186/s13059-016-0881-8.
- 668 Cuomo, C.A. *et al.* (2012) 'Microsporidian genome analysis reveals evolutionary strategies
669 for obligate intracellular growth', *Genome Research*, 22(12), pp. 2478–2488.
670 doi:10.1101/gr.142802.112.
- 671 Desjardins, C.A. *et al.* (2015) 'Contrasting host-pathogen interactions and genome evolution
672 in two generalist and specialist microsporidian pathogens of mosquitoes.', *Nature*
673 *communications*, 6, p. 7121. doi:10.1038/ncomms8121.
- 674 Di Tommaso, P. *et al.* (2011) 'T-Coffee: a web server for the multiple sequence alignment of
675 protein and RNA sequences using structural information and homology extension', *Nucleic*
676 *Acids Research*, 39(suppl), pp. W13–W17. doi:10.1093/nar/gkr245.
- 677 Eddy, S.R. (2011) 'Accelerated Profile HMM Searches', *PLOS Computational Biology*, 7(10), p.
678 e1002195. doi:10.1371/journal.pcbi.1002195.
- 679 Emms, D.M. and Kelly, S. (2019) 'OrthoFinder: phylogenetic orthology inference for
680 comparative genomics', *Genome Biology*, 20(1), p. 238. doi:10.1186/s13059-019-1832-y.
- 681 Engelmann, I. *et al.* (2011) 'A comprehensive analysis of gene expression changes provoked
682 by bacterial and fungal infection in *C. elegans*.', *PloS one*, 6(5), p. e19055.
683 doi:10.1371/journal.pone.0019055.
- 684 Ewels, P. *et al.* (2016) 'MultiQC: summarize analysis results for multiple tools and samples in
685 a single report', *Bioinformatics*, 32(19), pp. 3047–3048. doi:10.1093/bioinformatics/btw354.
- 686 Flores, J. *et al.* (2021) 'Human microsporidian pathogen *Encephalitozoon intestinalis*
687 impinges on enterocyte membrane trafficking and signaling', *Journal of Cell Science*, 134(5),
688 p. jcs253757. doi:10.1242/jcs.253757.
- 689 Grover, M. *et al.* (2021) 'Infection of *C. elegans* by Haptoglossa Species Reveals Shared
690 Features in the Host Response to Oomycete Detection', *Frontiers in Cellular and Infection*
691 *Microbiology*, 11, p. 973. doi:10.3389/fcimb.2021.733094.
- 692 Haag, K.L. *et al.* (2014) 'Evolution of a morphological novelty occurred before genome
693 compaction in a lineage of extreme parasites', *Proceedings of the National Academy of*
694 *Sciences*, 111(43), pp. 15480–15485. doi:10.1073/pnas.1410442111.
- 695 Huang, D.W., Sherman, Brad T. and Lempicki, R.A. (2009) 'Bioinformatics enrichment tools:
696 paths toward the comprehensive functional analysis of large gene lists', *Nucleic Acids*
697 *Research*, 37(1), pp. 1–13. doi:10.1093/nar/gkn923.
- 698 Huang, D.W., Sherman, Brad T and Lempicki, R.A. (2009) 'Systematic and integrative analysis
699 of large gene lists using DAVID bioinformatics resources', *Nature Protocols*, 4(1), pp. 44–57.
700 doi:10.1038/nprot.2008.211.

- 701 Huelsenbeck, J.P. and Ronquist, F. (2001) 'MRBAYES: Bayesian inference of phylogenetic
702 trees', *Bioinformatics*, 17(8), pp. 754–755. doi:10.1093/bioinformatics/17.8.754.
- 703 James, T.Y. *et al.* (2013) 'Shared Signatures of Parasitism and Phylogenomics Unite
704 Cryptomycota and Microsporidia', *Current Biology*, 23(16), pp. 1548–1553.
705 doi:10.1016/j.cub.2013.06.057.
- 706 Katinka, M.D. *et al.* (2001) 'Genome sequence and gene compaction of the eukaryote
707 parasite *Encephalitozoon cuniculi*.' *Nature*, 414(6862), pp. 450–453. doi:10.1038/35106579.
- 708 L. Goff, C.T. (2017) *Cummerbund: analysis, exploration, manipulation, and visualization of*
709 *cufflinks high-throughput sequencing data*. Bioconductor.
710 doi:10.18129/B9.BIOC.CUMMERBUND.
- 711 Langmead, B. and Salzberg, S.L. (2012) 'Fast gapped-read alignment with Bowtie 2', *Nature*
712 *Methods*, 9(4), pp. 357–359. doi:10.1038/nmeth.1923.
- 713 Lansdon, P., Carlson, M. and Ackley, B.D. (2022) 'Wild-type *Caenorhabditis elegans* isolates
714 exhibit distinct gene expression profiles in response to microbial infection', *BMC Genomics*,
715 23(1), p. 229. doi:10.1186/s12864-022-08455-2.
- 716 Lažetić, V. *et al.* (2022) 'The transcription factor ZIP-1 promotes resistance to intracellular
717 infection in *Caenorhabditis elegans*', *Nature Communications*, 13(1), p. 17.
718 doi:10.1038/s41467-021-27621-w.
- 719 Leyva-Díaz, E. *et al.* (2017) 'Silencing of Repetitive DNA Is Controlled by a Member of an
720 Unusual *Caenorhabditis elegans* Gene Family', *Genetics*, 207(2), pp. 529–545.
721 doi:10.1534/genetics.117.300134.
- 722 Li, H. *et al.* (2009) 'The Sequence Alignment/Map format and SAMtools', *Bioinformatics*,
723 25(16), pp. 2078–2079. doi:10.1093/bioinformatics/btp352.
- 724 Luallen, R.J. *et al.* (2016) 'Discovery of a Natural Microsporidian Pathogen with a Broad
725 Tissue Tropism in *Caenorhabditis elegans*', *PLoS pathogens*, 12(6), p. e1005724.
726 doi:10.1371/journal.ppat.1005724.
- 727 Ma, Z. *et al.* (2013) 'Genome-Wide Transcriptional Response of Silkworm (*Bombyx mori*) to
728 Infection by the Microsporidian *Nosema bombycis*', *PLOS ONE*, 8(12), p. e84137.
729 doi:10.1371/journal.pone.0084137.
- 730 Marini, F. and Binder, H. (2019) 'pcaExplorer: an R/Bioconductor package for interacting
731 with RNA-seq principal components', *BMC Bioinformatics*, 20(1), p. 331.
732 doi:10.1186/s12859-019-2879-1.
- 733 Mi, H. *et al.* (2021) 'PANTHER version 16: a revised family classification, tree-based
734 classification tool, enhancer regions and extensive API', *Nucleic Acids Research*, 49(D1), pp.
735 D394–D403. doi:10.1093/nar/gkaa1106.

- 736 Midttun, H.L.E. *et al.* (2020) 'Effects of Pseudoloma neurophilia infection on the brain
737 transcriptome in zebrafish (*Danio rerio*)', *Journal of Fish Diseases*, 43(8), pp. 863–875.
738 doi:10.1111/jfd.13198.
- 739 Murareanu, B.M. *et al.* (2021) 'Generation of a Microsporidia Species Attribute Database
740 and Analysis of the Extensive Ecological and Phenotypic Diversity of Microsporidia', *mBio*.
- 741 Nakjang, S. *et al.* (2013) 'Reduction and expansion in microsporidian genome evolution: new
742 insights from comparative genomics.', *Genome biology and evolution*, 5(12), pp. 2285–2303.
743 doi:10.1093/gbe/evt184.
- 744 Notredame, C., Higgins, D.G. and Heringa, J. (2000) 'T-coffee: a novel method for fast and
745 accurate multiple sequence alignment 1 Edited by J. Thornton', *Journal of Molecular
746 Biology*, 302(1), pp. 205–217. doi:10.1006/jmbi.2000.4042.
- 747 Pimentel, H. *et al.* (2017) 'Differential analysis of RNA-seq incorporating quantification
748 uncertainty', *Nature Methods*, 14(7), pp. 687–690. doi:10.1038/nmeth.4324.
- 749 Quandt, C.A. *et al.* (2017) 'The genome of an intranuclear parasite, Paramicrosporidium
750 saccamoebae, reveals alternative adaptations to obligate intracellular parasitism', *eLife*.
751 Edited by A. Rokas, 6, p. e29594. doi:10.7554/eLife.29594.
- 752 Reddy, K.C. *et al.* (2017) 'An Intracellular Pathogen Response Pathway Promotes
753 Proteostasis in *C. elegans*', *Current biology: CB*, 27(22), pp. 3544-3553.e5.
754 doi:10.1016/j.cub.2017.10.009.
- 755 Reddy, K.C. *et al.* (2019) 'Antagonistic paralogs control a switch between growth and
756 pathogen resistance in *C. elegans*', *PLoS pathogens*, 15(1), p. e1007528.
757 doi:10.1371/journal.ppat.1007528.
- 758 Reinke, A.W. *et al.* (2017) 'Identification of microsporidia host-exposed proteins reveals a
759 repertoire of rapidly evolving proteins.', *Nature communications*, 8, p. 14023.
760 doi:10.1038/ncomms14023.
- 761 Ronquist, F. and Huelsenbeck, J.P. (2003) 'MrBayes 3: Bayesian phylogenetic inference
762 under mixed models', *Bioinformatics*, 19(12), pp. 1572–1574.
763 doi:10.1093/bioinformatics/btg180.
- 764 Sinha, A. *et al.* (2012) 'System Wide Analysis of the Evolution of Innate Immunity in the
765 Nematode Model Species *Caenorhabditis elegans* and *Pristionchus pacificus*', *PLOS ONE*,
766 7(9), p. e44255. doi:10.1371/journal.pone.0044255.
- 767 Sowa, J.N. *et al.* (2019) 'The *Caenorhabditis elegans* RIG-I Homolog DRH-1 Mediates the
768 Intracellular Pathogen Response upon Viral Infection', *Journal of Virology* [Preprint].
769 doi:10.1128/JVI.01173-19.
- 770 Stein, L.D. *et al.* (2003) 'The genome sequence of *Caenorhabditis briggsae*: a platform for
771 comparative genomics.', *PLoS biology*, 1(2), p. E45. doi:10.1371/journal.pbio.0000045.

- 772 Stentiford, G.D. *et al.* (2016) 'Microsporidia – Emergent Pathogens in the Global Food
773 Chain', *Trends in Parasitology*, 32(4), pp. 336–348. doi:10.1016/j.pt.2015.12.004.
- 774 Szumowski, S.C. and Troemel, E.R. (2015) 'Microsporidia–host interactions', *Current Opinion
775 in Microbiology*, 26, pp. 10–16. doi:10.1016/j.mib.2015.03.006.
- 776 Tamim El Jarkass, H. and Reinke, A.W. (2020) 'The ins and outs of host-microsporidia
777 interactions during invasion, proliferation and exit', *Cellular Microbiology*, 22(11).
778 doi:10.1111/cmi.13247.
- 779 Tecle, E. *et al.* (2021) 'The purine nucleoside phosphorylase pnp-1 regulates epithelial cell
780 resistance to infection in *C. elegans*', *PLOS Pathogens*, 17(4), p. e1009350.
781 doi:10.1371/journal.ppat.1009350.
- 782 Tecle, E. and Troemel, E.R. (2022) 'Insights from *C. elegans* into Microsporidia Biology and
783 Host-Pathogen Relationships.', *Experientia supplementum (2012)*, 114, pp. 115–136.
784 doi:10.1007/978-3-030-93306-7_5.
- 785 Thomas, J.H. (2006) 'Adaptive evolution in two large families of ubiquitin-ligase adapters in
786 nematodes and plants', *Genome Research*, 16(8), pp. 1017–1030. doi:10.1101/gr.5089806.
- 787 Trapnell, C. *et al.* (2010) 'Transcript assembly and quantification by RNA-Seq reveals
788 unannotated transcripts and isoform switching during cell differentiation', *Nature
789 Biotechnology*, 28(5), pp. 511–515. doi:10.1038/nbt.1621.
- 790 Trapnell, C. *et al.* (2013) 'Differential analysis of gene regulation at transcript resolution with
791 RNA-seq', *Nature Biotechnology*, 31(1), pp. 46–53. doi:10.1038/nbt.2450.
- 792 Trapnell, C., Pachter, L. and Salzberg, S.L. (2009) 'TopHat: discovering splice junctions with
793 RNA-Seq', *Bioinformatics*, 25(9), pp. 1105–1111. doi:10.1093/bioinformatics/btp120.
- 794 Troemel, E.R. *et al.* (2008) 'Microsporidia are natural intracellular parasites of the nematode
795 *Caenorhabditis elegans*.' *PLoS biology*, 6(12), pp. 2736–2752.
796 doi:10.1371/journal.pbio.0060309.
- 797 Vávra, J. and Lukeš, J. (2013) 'Chapter Four - Microsporidia and "The Art of Living Together"',
798 in Rollinson, D. (ed.) *Advances in Parasitology*. Academic Press, pp. 253–319.
799 doi:10.1016/B978-0-12-407706-5.00004-6.
- 800 Wadi, L. and Reinke, A.W. (2020) 'Evolution of microsporidia: An extremely successful group
801 of eukaryotic intracellular parasites', *PLOS Pathogens*. Edited by L.J. Knoll, 16(2), p.
802 e1008276. doi:10.1371/journal.ppat.1008276.
- 803 Wang, L., Wang, S. and Li, W. (2012) 'RSeQC: quality control of RNA-seq experiments',
804 *Bioinformatics*, 28(16), pp. 2184–2185. doi:10.1093/bioinformatics/bts356.
- 805 Willis, A.R. *et al.* (2021) 'A parental transcriptional response to microsporidia infection
806 induces inherited immunity in offspring', *Science Advances*, 7(19), p. eabf3114.
807 doi:10.1126/sciadv.abf3114.

- 808 Willis, A.R. and Reinke, A.W. (2022) 'Factors That Determine Microsporidia Infection and
809 Host Specificity.', *Experientia supplementum (2012)*, 114, pp. 91–114. doi:10.1007/978-3-
810 030-93306-7_4.
- 811 Wong, D. *et al.* (2007) 'Genome-wide investigation reveals pathogen-specific and shared
812 signatures in the response of *Caenorhabditis elegans* to infection', *Genome Biology*, 8(9), p.
813 R194. doi:10.1186/gb-2007-8-9-r194.
- 814 Zárte-Potes, A. *et al.* (2020) 'The *C. elegans* GATA transcription factor elt-2 mediates
815 distinct transcriptional responses and opposite infection outcomes towards different
816 *Bacillus thuringiensis* strains', *PLOS Pathogens*, 16(9), p. e1008826.
817 doi:10.1371/journal.ppat.1008826.
- 818 Zhang, G. *et al.* (2016) 'A Large Collection of Novel Nematode-Infecting Microsporidia and
819 Their Diverse Interactions with *Caenorhabditis elegans* and Other Related Nematodes', *PLOS*
820 *Pathogens*. Edited by J.B. Lok, 12(12), p. e1006093. doi:10.1371/journal.ppat.1006093.
- 821
822